

Geo-Congress 2026

GSP 380

Geoenvironmental Engineering, Sustainability, and Coastal Geotechnics

Selected Papers from Geo-Congress 2026
Salt Lake City, Utah | March 9–12, 2026

Edited by

Jack Montgomery, Ph.D., P.E.
Brady R. Cox, Ph.D., P.E.

ASCE

G-I GEO-INSTITUTE

GEOTECHNICAL SPECIAL PUBLICATION NO. 380

GEO-CONGRESS 2026

GEOENVIRONMENTAL ENGINEERING, SUSTAINABILITY, AND COASTAL GEOTECHNICS

SELECTED PAPERS FROM SESSIONS OF GEO-CONGRESS 2026

March 9–12, 2026
Salt Lake City, Utah

SPONSORED BY

The Geo-Institute
of the American Society of Civil Engineers

EDITED BY
Jack Montgomery, Ph.D., P.E.
Brady R. Cox, Ph.D., P.E.

Published by the American Society of Civil Engineers

Published by American Society of Civil Engineers
1801 Alexander Bell Drive
Reston, Virginia, 20191-4382
www.asce.org/publications | ascelibrary.org

Any statements expressed in these materials are those of the individual authors and do not necessarily represent the views of ASCE, which takes no responsibility for any statement made herein. No reference made in this publication to any specific method, product, process, or service constitutes or implies an endorsement, recommendation, or warranty thereof by ASCE. The materials are for general information only and do not represent a standard of ASCE, nor are they intended as a reference in purchase specifications, contracts, regulations, statutes, or any other legal document. ASCE makes no representation or warranty of any kind, whether express or implied, concerning the accuracy, completeness, suitability, or utility of any information, apparatus, product, or process discussed in this publication, and assumes no liability therefor. The information contained in these materials should not be used without first securing competent advice with respect to its suitability for any general or specific application. Anyone utilizing such information assumes all liability arising from such use, including but not limited to infringement of any patent or patents.

ASCE and American Society of Civil Engineers—Registered in U.S. Patent and Trademark Office.

Photocopies and permissions. Permission to photocopy or reproduce material from ASCE publications can be requested by sending an e-mail to permissions@asce.org or by locating a title in ASCE's Civil Engineering Database (http://cedb.asce.org) or ASCE Library (http://ascelibrary.org) and using the "Permissions" link.

Errata: **Errata, if any, can be found at https://doi.org/10.1061/9780784486757**

Copyright © 2026 by the American Society of Civil Engineers.
All Rights Reserved.
ISBN 978-0-7844-8675-7 (PDF)
Manufactured in the United States of America.

Preface

This is the sixth volume of seven Geotechnical Special Publications (GSPs) containing papers from Geo-Congress 2026: Geo Tools, Technologies, and Techniques in an Environment of Change, held in Salt Lake City, Utah, on March 9-12, 2026. Notably, this conference marks the 30th anniversary of the Geo-Institute. The conference brought together industry leaders, researchers, and practitioners to showcase innovations, address critical challenges, and advance knowledge in geotechnical engineering. The conference hosted the Terzaghi, Peck, Seed, and Prakash Lectures and many technical sessions, panel sessions, short courses, and student competitions.

These proceedings represent the culmination of nearly two years of effort by the program committee and many other individuals, whose focus has been to continue the success of previous Geo-Congresses and to celebrate 30 years of geotechnical innovation by the Geo-Institute. Building the program started with an international call for papers that resulted in more than 800 abstracts on a variety of important topics. Each paper was subjected to a rigorous technical review by two or more independent peer reviewers. Acceptance required concurrence by at least two peer reviewers, and final decisions were made only after review coordinators confirmed that authors satisfactorily addressed any reviewer comments on their original submission. All accepted papers are presented at the conference as posters or technical talks and are eligible for applicable ASCE awards.

This volume contains a collection of 53 papers focused primarily on the topics of geoenvironmental engineering, sustainability, and geotechnical engineering in coastal environments. This includes papers on landfills, sustainable soil improvement, the use of recycled materials, and wave loading.

The success of this conference and proceedings would not have been possible without the participation and collaboration of many individuals, including Brad Keelor, the tireless staff at the Geo-Institute, and the many session chairs and reviewers. We hope that these proceedings will be of use to the geotechnical engineering community for many years to come.

The Editors,

Jack Montgomery, Ph.D., P.E., M.ASCE, Auburn University
Brady R. Cox, Ph.D., P.E., M.ASCE, Utah State University

© ASCE

Acknowledgments

We are very grateful for the contributions of the authors, peer reviewers, session chairs, and program committee, without whom this publication would not be possible.

Geo-Congress 2026 Conference Program Committee

Conference Chairs
K. N. Gunalan, Ph.D., P.E., BC.GE, Pres. 20 ASCE, NAC, HNTB Corporation
Ryan B. Maw, P.E., G.E., BC.GE, F.ASCE, Gerhart Cole

Technical Chair
Shideh Dashti, Ph.D., M.ASCE, University of Colorado Boulder

Proceedings Editors
Brady R. Cox, Ph.D., P.E., M.ASCE, Utah State University
Jack Montgomery, Ph.D., P.E., M.ASCE, Auburn University

Student Program Liaison
Cassandra Rutherford, Ph.D., P.E., M.ASCE, Iowa State University

Program Committee Members
Aaron L. Leopold, P.E., M.ASCE, Dan Brown and Associates
Kam Ng, Ph.D., P.E., M.ASCE, University of Wyoming
Jenny Ramirez, Ph.D., P.E., M.ASCE, Geosyntec Consultants

© ASCE

Contents

Coastal Geotechnics

Comparison of Sandy Beach Moisture Content Measurements from In Situ Sampling and Moisture Probes 1
Julie Paprocki and Muhammad Touqeer

Evaluating the Efficacy of Instrumented Settlement Plates (ISP) in Monitoring Geotechnical Properties of Dredged Sediments in Marsh Creation Projects 10
Omar Snosi and Navid Jafari

Fluid-Soil Interaction Observations from a Dam-Break Wave Generator Using the University of Colorado Boulder's 400 G-Ton Centrifuge 18
Angela Mink, Srikanth S. C. Madabhushi, and Shengzhe Wang

Hydraulic Conductivity of Trench Backfills as a Mitigation Strategy for Chloride-Induced Corrosion in Coastal Iron Pipelines 28
E. Issmaeel, C. Harris, M. Gabr, M. Pourghaz, G. Lucier, and S. Almuaythir

Improving Containment Dike Stability with Geosynthetics: A Study on Louisiana Coastal Soils 38
Abhishek K. Tiwari, Udaya Panta, and Jay X. Wang

Large-Scale Wave Flume Experiments for Modeling Coastal Seabed under Solitary Waves 49
Ahmad Klait, Seyedalireza Mirghafouri, Majid Ghayoomi, Ali Farhadzadeh, and Tian-Jian Hsu

Measuring the Shear Strength of *Spartina alterniflora* Vegetated Soil in Delaware Salt Marshes Using Field Vane Shear Tests 59
Siamak Yoosefi, Christopher L. Meehan, Mohammadamin Nozari, and Claudia Zoccarato

Numerical Modeling of Artificial Mangrove Systems for Unprotected Earthen Embankment for Protection against Wave-Induced Erosion and Overtopping 68
Ayush Kumar, Vinay Krishnan, and Anand J. Puppala

Pore Pressure Assessment in Sandy Nearshore Sediments during a Large-Scale Wave Flume Experiment 79
Lea A. Eggensberger, Nina Stark, and Jack A. Puleo

© ASCE

Shear Behavior of Mangrove Soils in Louisiana and Texas: A Dual Approach Using Large-Scale Direct Shear Testing and In Situ Cone Penetration Testing 89
Mohamed Hassan, Hamed Nasiri, Youssef Mousa, Andre Rovai, Ivan Lopez, Aaron Meyers, Jorge A. Pineda Gomez, Xiaochen Zhao, Daniel J. Jensen, Annemarie E. Peacock, Anna R. Armitage, Jaime Brinkley, Briana Sebastian, Jacob Berkowitz, Marc Simard, Robert Twilley, and Navid Jafari

Supporting Coastal Shorelines through Site Characterization of a Confined Dredged Material Disposal Facility in Southern New Jersey 99
Daniel Gallegos, Justin Shawler, Brian Harris, Kaitlyn McPherran, David White, Jonathan Hubler, and Monica Chasten

Education for Geotechnical Engineering

Approaches to Teaching Geoenvironmental Engineering to Non-Geotechnical Engineers 113
Jean Benoît

Geoenvironmental Engineering

Chloride Corrosion and Earth Retaining Systems: Measurement and Calibration Techniques to Track Chloride Movements in Soils 125
Jenna Stein, Srikanth S. C. Madabhushi, and Ronald Y. S. Pak

Compressibility and Volume Change of Bentonite at Variable Temperatures 134
Abdallah Almajed, Muawia Dafalla, and Kehinde Lemboye

Data-Driven Machine Learning Surrogates to CTHBM Model for MSW Landfill Settlement Prediction 142
Jagadeesh Kumar Janga and Krishna R. Reddy

Effect of Plasticity Index on the Spatiotemporal Evolution of Desiccation-Induced Strain Localization in Compacted Clayey Soils Using DIC 153
Soumik Majumder and Ajanta Sachan

Efficacy of Construction and Demolition Waste on the Strength Enhancement of Expansive Soil: An Experimental Exploration 164
Shailesh Kumar Yadav, Amaan Hussain, and Ramakrishna Bag

Engineering Considerations and Case Histories of Landfill Intermediate Covers 174
Ming Zhu and Bryan Scholl

© ASCE

Enhanced Shear Strength of Wildfire Impacted Soils Using Biochar and Chitosan **185**
Krishna R. Reddy, Banuchandra Nagaraja, Jagadeesh Kumar Janga, and Arvin Farid

Enhancing the Chemical Compatibility of Calcium Bentonite-Soil Vertical Barrier through Biostimulated MICP **196**
Yu Zhang and Ningjun Jiang

Enhancing the Properties of Landfill-Mined Legacy Soil-Like Fine Fractions through Local Soil Blending: A Novel Approach **205**
Pradyumna Konar, Satyendra Mittal, and Absar Ahmad Kazmi

Field Performance of Compacted Amended Clay Liners at an Industrially Polluted Site **215**
Jialei Wan, Jiaming Wen, Yingzhen Li, Chi Che, and Yanjun Du

Geotechnical Assessment of Dredged Sediments as an Infiltration Berm Medium **227**
Eren Kaya, Adam Smith, Allen P. Davis, and Ahmet H. Aydilek

Modeling Solute Transport through Semipermeable Bentonite-Based Barriers under Transient Conditions **239**
Andrea Dominijanni and Nicolò Guarena

Novel Biogeochemical Cover for Landfill Gas Mitigation: Insights into Microbial Diversity **249**
Gaurav Verma and Krishna R. Reddy

Phytoremediation Potential of Diesel Contaminated Soil Using Selected Grass Species **260**
S. A. Abdul-Basit, J. Ochepo, T. S. Ijimdiya, A. O. Eberemu, and K. J. Osinubi

Sediment ISS in an Aqueous Environment: An Innovative Adaptation of a Proven Remedial Technique **273**
Darin Payne, Ken Andromalos, Angelo Toscano, Nathan Coughenour, and Michelina Ponziani

Sorption Performance of Sandy Clay Soil Using Duraflex as a Cement Admixture against Iron Contamination **283**
Jonny Mercedes and Giancarlo Flores

Stabilization of Construction and Demolition Waste with High Fines Content Using Biopolymer **296**
Beatrice Magombana, Shihui Liu, Kang Du, and Lin Li

© ASCE

Static and Cyclic Behavior of Oil Contaminated Sand 304
Anjali Verma and Nihar Ranjan Patra

Sustainable Utilization of Waste Slurry in Road Construction: Development and Evaluation of Solidification Methods Using Industrial Byproducts.....315
Xuanyu Chen, Bowen Yu, and Ningjun Jiang

Swelling Ratio of a Hydrophilic Seal and Flow Rates of the Interlocking System in Composite Geomembrane Cutoff Walls Exposed to Metal-Rich Solutions.....325
Min Wang, Xian-Lei Fu, and Yan-Jun Du

Testing Considerations for Quantifying PFAS Adsorption by a Soil-Bentonite Matrix Amended with Granular Activated Carbon.....336
Leeann Michael, Kevin Gilmore, Michael Malusis, and Austin Wadle

Water Repellent Soils in Geoenvironmental Applications.....346
Micheal Uduebor, Vincent Ogunro, and John Daniels

Sustainability in Geotechnical Engineering

Application of Phase Change Material in Enhancing the Efficiency of Geothermal Energy Piles.....357
Sohail Saheb, Omid Ghasemi-Fare, and Mark McGinley

Application of Sole Shallow Geothermal Systems for Deicing and Enhancing the Resilience of Existing Bridge Decks: A Field Testing Approach 368
Amin Mohammadzadeh, Mir Ali Hosseini, Omid Ghasemi-Fare, and Zhihui Sun

Centrifuge Modeling of the Effects of Native Vegetation on Levee Slope Stability.....377
Nethmi Silva, Tommy D. Bounds, April Bowman, and Kanthasamy K. Muraleetharan

Characterization of Recycled Materials for Advancing Sustainable Utilization into Transportation Geotechnical Infrastructure.....388
Balaji Lakkimsetti, Shanmukha Sai Avinash Gonnabathula, and Anand J. Puppala

Coal Fly Ash-Based Passive Treatment of Acid Mine Drainage 398
Masrur Mahedi, Bora Cetin, Kaoru Ikuma, and Rayla Pinto-Vilar

Durability Evaluation of Soil-Geopolymer Based Composites for 3D Printing Applications in Geotechnical Engineering 409
Akash Ashok Tanshette, Zoheb Faisal, Jianxin Huang, and Anand J. Puppala

© ASCE

Dynamic LCA Framework for Environmental Impact Assessment of a Tunnel in Northwestern China 422
Xinlei Hu and Ningjun Jiang

Early Detection of Slope Deformation Using Airborne LiDAR Monitoring 431
M. F. Khan, A. Q. M. Zohuruzzaman, S. Khan, and I. LaCour

Evaluating the Durability and Recycling Potential of Xanthan Gum-Amended Soils for Sustainable Geotechnical Infrastructure 439
Alek Zhang, Prince Jed Catacutan, Pania Newell, and Marta Miletić

Evaluation of Printability and Flow Properties of 3D-Printed Earthen Mixes 450
Saswati Ray, Md. Montaseer Meraz, Pavan Akula, John Rushing, and Jeb S. Tingle

Feasibility of Geothermal Energy Pile Use in Alluvial Deposits in New Orleans 461
Patrick A. Thurmond

Innovative Approaches to Addressing Surficial Slope Failures: The Role of Engineered Earth Armoring Solutions in Enhancing Infrastructure Resiliency 472
Jared Hill and Drew Loizeaux

Large-Scale Carbonation of Recycled Concrete Aggregates (RCA): Aggregate Properties and Implications to Transportation Geotechnics 483
Hossein Sousanabadi Farahani, Chris Hawkins, Jiong Hu, Eric Thompson, and Seunghee Kim

Multiscale Analysis of Water Stability and Durability of High-Dosage Phosphogypsum Subgrade Fillers in Water-Rich Environments 494
Zihao Hu, Qianwei Ma, Huaming Lu, and Ningjun Jiang

Performance Evaluation of Virgin and Recycled Aggregate Blends for Unpaved Roads under Freeze-Thaw Cycles 505
Umar Farooq, Celso Santos, Bora Cetin, Jeramy Ashlock, and Mahsa Belalzadeh

Strain-Dependent Effects of Microplastic Contamination on the Strength and Modulus of Kaolin Clay 517
Brandon De Jesus, Elizabeth Nunez, and Wing Shun Kwan

Strengthening Recycled Glass Sand Using Xanthan Gum: A Sustainable Approach 528
Junjie Li, Kejun Wen, and Bin Zhang

© ASCE

Sustainability Analysis of MICP-Treated High-Fines Soil with Geocell Reinforcement for Pavement Base Stability 538
Mabin Dahal, Bhaskar C. S. Chittoori, and Nick Hudyma

Sustainability Benefits Assessment of Cement and Recycled Concrete Aggregate Fines in Subgrade Stabilization Application 548
Muddassir Sanei, Nripojyoti Biswas, Jianxin Huang, and Anand J. Puppala

© ASCE

Comparison of Sandy Beach Moisture Content Measurements from In Situ Sampling and Moisture Probes

Julie Paprocki, Ph.D., P.E.[1]; and Muhammad Touqeer[2]

[1]Dept. of Civil and Environmental Engineering, Univ. of New Hampshire, Durham, NH.
Email: julie.paprocki@unh.edu
[2]Dept. of Civil and Environmental Engineering, Univ. of New Hampshire, Durham, NH.
Email: muhammad.touqeer@unh.edu

ABSTRACT

Moisture content is a critical strength parameter for estimating the strength of sandy beach soils. Recent work has explored the use of satellite-based remote sensing for deriving maps of moisture content. The use of remote sensing, however, requires accurate and reliable field measurements for calibration. Conductivity moisture probes have emerged as popular methods to measure the in situ moisture content. These probes rely on accurate calibration for the soil type, density, and salinity to provide accurate measurements of moisture content. This study compares moisture contents derived from a conductivity moisture probe to those derived from soil sampling to assess if a single set of calibration constants can be used to accurately estimate the moisture content across the entire beach profile. The volumetric moisture contents derived from moisture probes resulted in consistent overestimates of the moisture content when compared to those derived from sediment sampling. Differences ranged from 0.9 to 7.1%, with greater overestimates observed in the foreshore, where higher unit weights were observed (15.2–16.9 kN/m^3). The results suggest that a single set of calibration constants is likely not sufficient to estimate the moisture content of dynamic environments, and factors such as differences in the unit weight, sand layering, grain sizes, and water salinity need to be accounted for when employing conductivity probes.

INTRODUCTION

Moisture content is a critical strength parameter for estimating the strength of partially saturated sandy soils for applications related to sediment transport and beach mobility. However, given the spatiotemporal variation of moisture content at sandy beaches as a result of waves, tides, and rainfall, there is a need for tools to develop spatial maps of moisture content. Recently, high resolution satellite-based remote sensing has emerged as a viable platform to develop these maps (Paprocki et al. 2022, 2023). The use of satellite systems, however, requires calibration using accurate, reliable, and repeatable field measurements of moisture content.

Moisture content has traditionally been measured using carefully collected in situ samples that are sealed and then transported to a laboratory for testing. Physical sampling allows for other relevant geotechnical properties, including grain sizes, unit weights, relative densities, and void ratios to be measured and permits soil characterization. The collection of these samples can be time-consuming, limiting the number of samples that can be easily collected. A loss of moisture content may also occur during the transport process if samples are not carefully sealed. Traditionally, the moisture content derived from physical samples is reported as the gravimetric moisture content (GMC), mc, and is expressed as a percentage:

© ASCE

$$mc = \frac{W_w}{W_s} \cdot 100 \quad (1)$$

where W_w and W_s are the weights of water and solids, respectively.

Conductivity moisture probes (Atherton et al. 2001; Davidson-Arnott et al. 2008; Namikas et al. 2010; Schmutz and Namikas 2011; Wiggs et al. 2004; Yang and Davidson-Arnott 2005; Zhu 2007) have also been proposed for measuring the volumetric moisture content (VMC), m_v, of beach sands:

$$m_v = \frac{V_w}{V_t} \quad (2)$$

where V_w and V_t are the volume of water and the total volume, respectively. Moisture probes operate on the fact that water has a high dielectric constant relative to the other materials (soil particles and air) within a soil sample (Hillel 1998). As soils are multiphase system composed of soil particles, air, and water (Lambe and Whitman 1969), the dielectric constant of the soil matrix is a composite of the dielectric constants of the individual parts. Individually, water, air, and soil have dielectric constants of ~80, 4, and 1, respectively. Since the dielectric constant of water is greater than the other two components, the overall dielectric constant of the mixture can be used to determine m_v of the soil.

Moisture probes, which are traditionally used to monitor the moisture content of freshwater agricultural fields, are calibrated for freshwater environments, which are usually provided by the manufacturer. Most probes, however, are not explicitly calibrated for saltwater, which has different dielectric properties than freshwater. To combat this impact, custom calibration factors can be developed (Brilli et al. 2022). Calibration factors are typically developed for a fixed soil unit weight and fluid composition (i.e., salinity level) over different moisture contents as the sample dries (Delta-T Devices Ltd 2016); this implies that calibration factors are dependent on soil density. For sandy beaches, where the unit weight of soils is highly variable due to compaction from waves and tides (Heathershaw et al. 1981) as well as loosening from anthropogenic action or aeolian driven transport, a single set of calibration factors may be insufficient to accurately estimate the moisture content across the beach profile.

This study aims to investigate the applicability of calibration constants required to convert moisture probe measurements to moisture contents across beach zones where the grain size and unit weight are variable. To test if multiple calibration factors are required to accurately estimate the moisture content from moisture probe measurements, observations of moisture content from the moisture probe were coupled with carefully collected sediment samples wherein the VMC is measured. These measurements were collected within three distinct beach zones (backshore, foreshore, and swash zone), representing a range of moisture content and unit weights.

METHODS

Field measurements were conducted at Wallis Sands State Beach, located in Rye, New Hampshire (43°1'37.95"N, 70°43'43.12"W; Figure 1), on November 21, 2024. Sampling occurred at approximately low tide. Wallis Sands has semidiurnal tides, a mean tidal range of 2.63 m, and beach profile widths of 130-160 m (Ward et al. 2021b). The sands are composed of quartz, feldspar, mica, and various metamorphic fragments (Tuttle 1960). Concurrent sediment samples and moisture probe measurements were collected at the nine stations shown in Figure 1b

© ASCE

along a single cross-shore transect. The position and elevation of each station was recorded using an Emlid Reach RS3 RTK GNSS receiver. Four stations (WS1-WS4) were located in the backshore (zone between the high water line during spring tides and the coastline and is normally dry), four (WS5-WS8) were located within the foreshore (zone between the regular tidal levels and is regularly covered and uncovered by water), while WS9 was located within the swash zone (zone that is regularly covered and uncovered by waves).

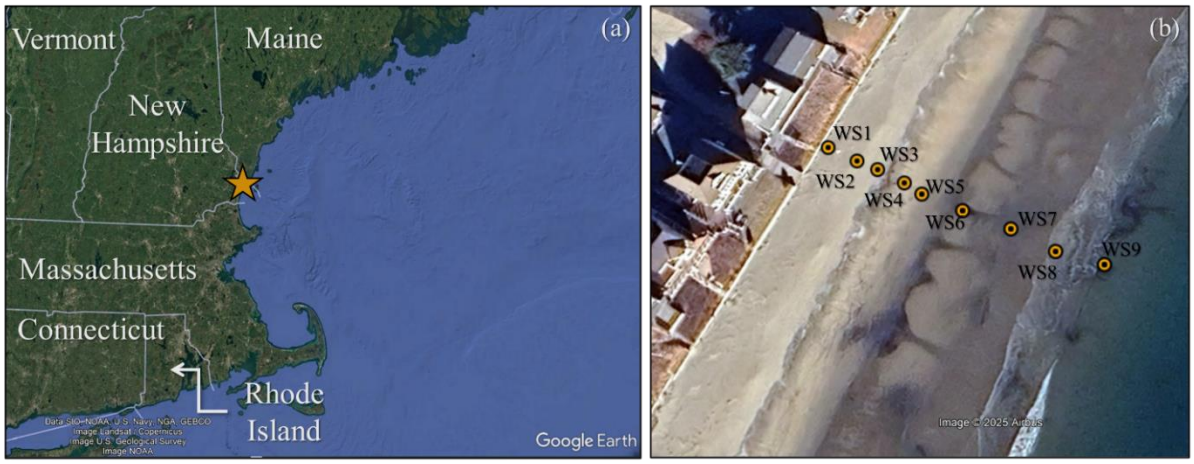


Figure 1. (a) Location of Wallis Sands State Beach in the Seacoast region of New Hampshire (orange star); (b) Cross-shore transect, with sampling locations denoted as orange circles.

The moisture probe used in this study, the Dynamax SM150T, is shown in Figure 2a. This probe was selected due to its ruggedness and its relative ease of use. To collect moisture readings, the SM150T is first pushed into the ground until the stainless steel rods are fully inserted. Power is then applied, and a 100 MHz waveform is created. This wave is applied to the rods, transmitting an electromagnetic field into the soil. The SMT150T then detects the voltage output that can then be converted to moisture content (Delta-T Devices Ltd 2016).

At each station, three moisture probe measurements were recorded and averaged together. Although the probe was advertised to be insensitive to changes in salinity (Delta-T Devices Ltd 2016), previous work has demonstrated that the salinity from seawater results in overestimates of the moisture content when using built-in calibration constants (Brilli et al. 2022). Therefore, measurements were recorded in mV and then converted to moisture content using custom calibration constants for sand based on the salinity (Brilli et al. 2022). For this study, the salinity was assumed to be 30 pss.

Physical soil samples were carefully collected using ~10 cm tall by 6.67 cm diameter tubes; an example is shown in Figure 2b. The soil samples were processed in the laboratory for unit weights, grain sizes, and moisture contents. Total unit weights were calculated using the total wet weight of the material in the tube and the volume of each tube. The total unit weights were then converted to dry unit weights using the measured moisture contents. To determine grain sizes and gravimetric moisture contents, each sample was divided into two 5 cm subsamples (one representing the top 5 cm, one representing the bottom 5 cm). Grain sizes were measured following ASTM D6913 (ASTM 2017a), with samples sieved using the 3/8”, No. 4, No. 10, No. 20, No. 40, No. 80, No. 100, and No. 200 sieves. Gravimetric moisture contents were recorded

© ASCE

by weighing the subsamples before and after drying overnight in an oven at 100 °C. The gravimetric moisture contents were converted to volumetric moisture contents using the bulk density (ratio of the mass of solids to the total volume of material), ρ_b:

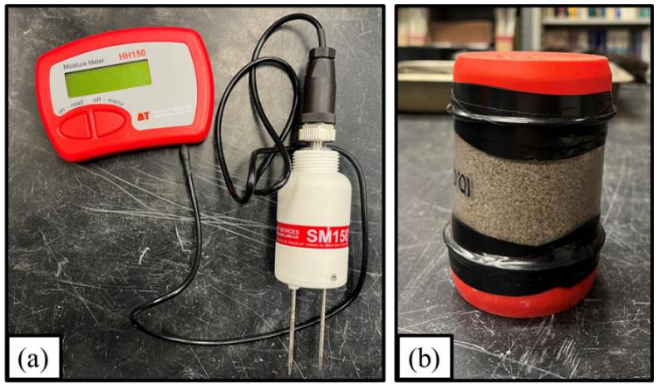


Figure 2. (a) The SM150T soil sensor; and (b) example soil sample.

$$mc = m_v \cdot \frac{\rho_w}{\rho_b} \quad (3)$$

where ρ_w is the density of water. For this study, it was assumed that ρ_w = 1025 kg/m^3 to account for the impacts of saltwater.

RESULTS AND DISCUSSION

The cross-shore trends in the dry unit weights are shown in Figure 3 and summarized in Table 1 for each station. The lowest values of dry unit weight were recorded in the foreshore (first four samples), with dry unit weights of 14.5-15.0 kN/m^3 (average of 14.8 kN/m^3). Within the foreshore, the dry unit weights ranged from 15.3-16.9 kN/m^3 (average of 16.0 kN/m^3). At WS5, where sampling transitions to the foreshore, the dry unit weight was 16.2 kN/m^3, which was the second highest value observed. The dry unit weights then decreased until WS7 before increasing again as sampling approached the water line. The peak dry unit weight was observed at WS9 (16.9 kN/m^3), corresponding to the swash zone at the time of measurements. Wave action can densify sediments (Heathershaw et al. 1981). This indicates that there should be higher unit weights within the foreshore (which is cyclically covered and uncovered with water during the tidal cycle and therefore, experiences densification by waves) and the highest values should be within the swash zone (which is actively being densified by waves). The lowest values, therefore, should be from the backshore, which was observed here. Using a specific gravity of 2.7, void ratios ranged from 0.57 in the swash zone to 0.83 at WS2 within the backshore.

The grain size distribution curves are presented in Figure 4. All samples classified poorly-graded (SP) sands following the Unified Soil Classification System (USCS) (ASTM D2487; ASTM 2017b). From these curves, the bottom 5 cm subsample was generally slightly coarser than the top subsample (differences in d_{50} of 0.008-0.15 mm); this is emphasized by the cross-shore variation in the median grain size, d_{50} (Figure 5). The top 5 cm of each sample exhibited d_{50} between 0.3-0.4 mm while the bottom 5 cm exhibited more variability in d_{50}. The greatest

© ASCE

difference occurred at WS6, with a difference of 0.15 mm. These trends in grain sizes and layering are consistent with previous observations at Wallis Sands (Ward et al. 2016, 2021a). A summary of the median grain sizes for each station is presented in Table 1.

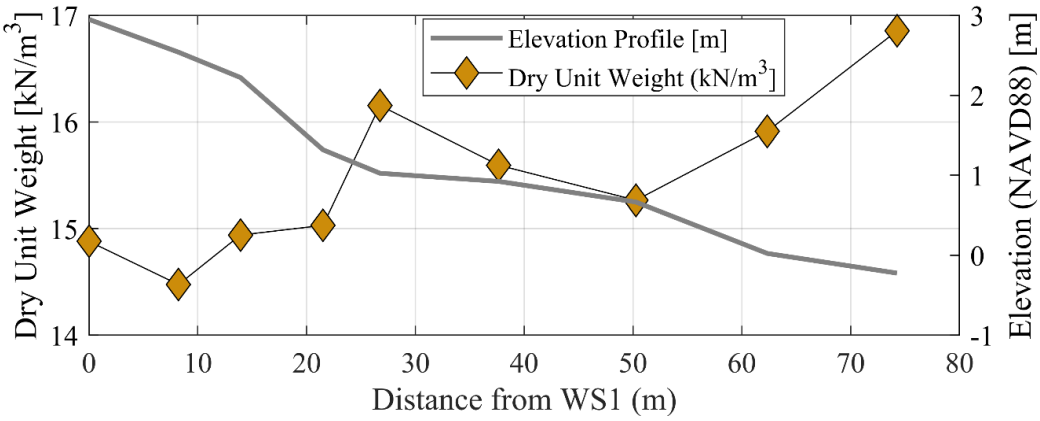


Figure 3. Cross-shore variation in the dry unit weight.

Table 1. Summary of in situ soil properties.

Station No.	Dry Unit Weight (kN/m^3)	d_{50} (mm)		Volumetric Moisture Content (%)	
		Top 5 cm of sample	Bottom 5 cm of sample	Moisture Probe	Soil Sample
WS1	14.9	0.37	0.36	3.5	4.6
WS2	14.5	0.36	0.34	6.8	7.9
WS3	14.9	0.39	0.34	9.3	10.7
WS4	15.0	0.44	0.37	20.8	22.6
WS5	16.2	0.41	0.39	31.6	35.2
WS6	15.6	0.52	0.37	30	31.7
WS7	15.3	0.35	0.34	29.3	35.2
WS8	15.9	0.37	0.36	28.9	36.9
WS9	16.9	0.39	0.36	30.7	35.9

The cross-shore variation in the moisture content is presented in Figure 6. The lowest gravimetric moisture contents (squares in Figure 6) occurred within the backshore (3.1%-14.8%), with a gradual increase while approaching the foreshore. Light rain was observed during field measurements, resulting in slightly elevated moisture contents beyond the typical values expected for the backshore. Within the foreshore, the moisture content remained approximately constant (19.9%-22.8%). A small decrease in the moisture content was observed at WS6, which corresponds to greatest median grain size (Figure 5). A summary of the moisture contents from the probe and soil samples for each station is presented in Table 1.

The volumetric moisture contents, both from the probe (triangles) and soil sampling (diamonds), exhibited the same patterns and trends as the gravimetric moisture contents, albeit with different values. The volumetric moisture contents from the soil samples always exceed those estimated using the moisture probe (Figures 6 and 7), with overestimates ranging from 0.9-

© ASCE

7.1%. The moisture contents from the backshore were underestimated by 1.0-1.3%, well within the reported accuracy of the SM150T probe (±3%; Delta-T Devices Ltd 2016).

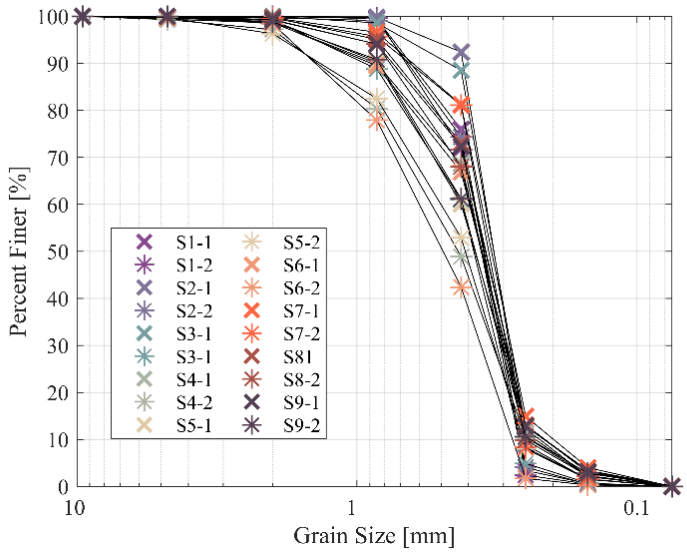


Figure 4. Grain size distributions.

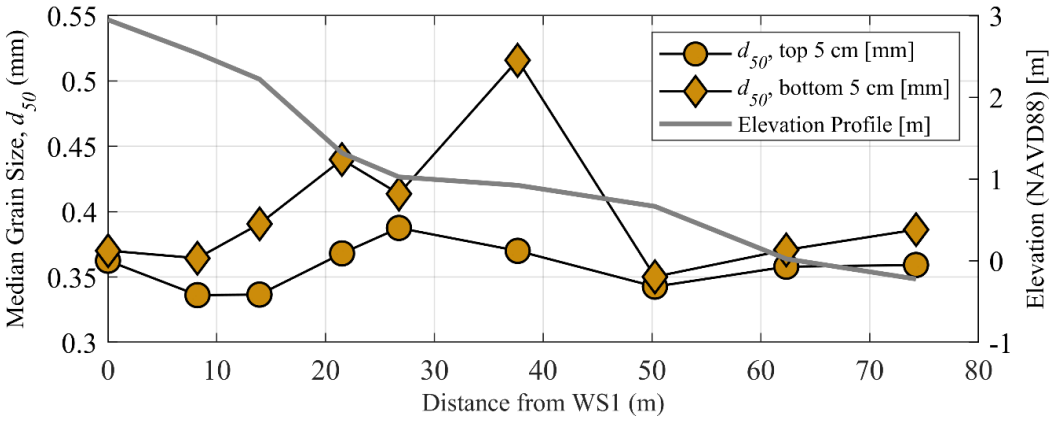


Figure 5. Cross-shore variation in median grain size, d_{50}, for the top 5 cm (circles) and the bottom 5 cm (diamonds) of the samples.

The greatest differences between the volumetric moisture content from the probe and sample occurred at the stations within the foreshore (overestimates of 0.9-7.1%), which exceeds the reported accuracy of the probe (±3%). In general, mismatches between the probe and sample volumetric moisture content occurred where the dry unit weight exceeded 15 kN/m^3. This suggests that a single set of calibration constants is likely insufficient to accurately measure the moisture content in a range of beach zones and that different calibration constants should be developed based on the dry unit weight. Station WS6, although within the foreshore, exhibited overestimates similar in magnitude to stations WS1-WS4 but exhibited a dry unit weight (15.6 kN/m^3) similar to the rest of the foreshore. The bottom 5 cm of the sample from WS6 was

© ASCE

coarser than the top 5 cm of the sample, suggesting that grain size likely impacts the measured moisture contents using the probe. When different grain sizes are present in distinct layers or patches on the beach, this results in a different volume of voids that are available to be filled with water. Future work will focus on understanding the impact of grain size and sediment layer on moisture probe measurements.

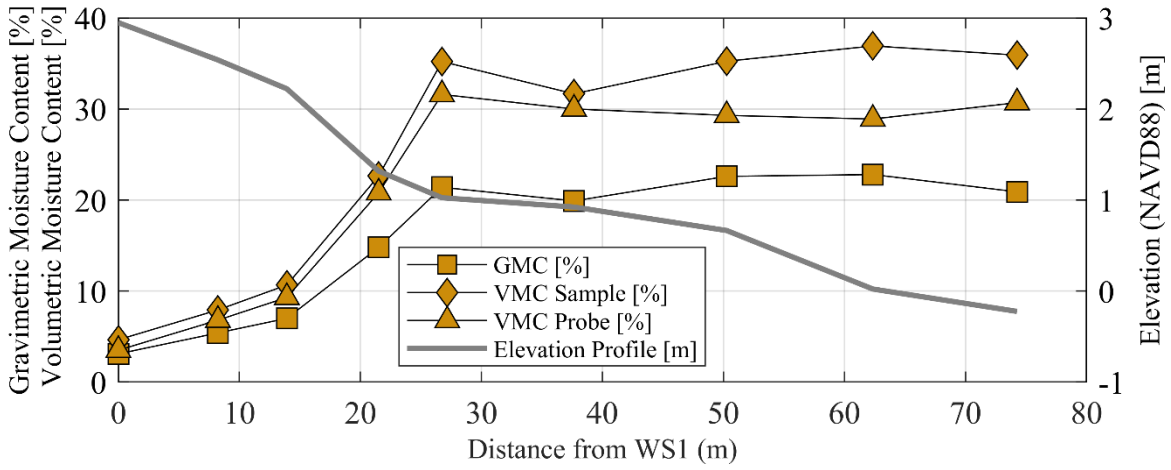


Figure 6. Cross-shore variation in the gravimetric moisture content (squares), volumetric moisture content from the samples (diamonds), and volumetric moisture content from the moisture probe (triangles).

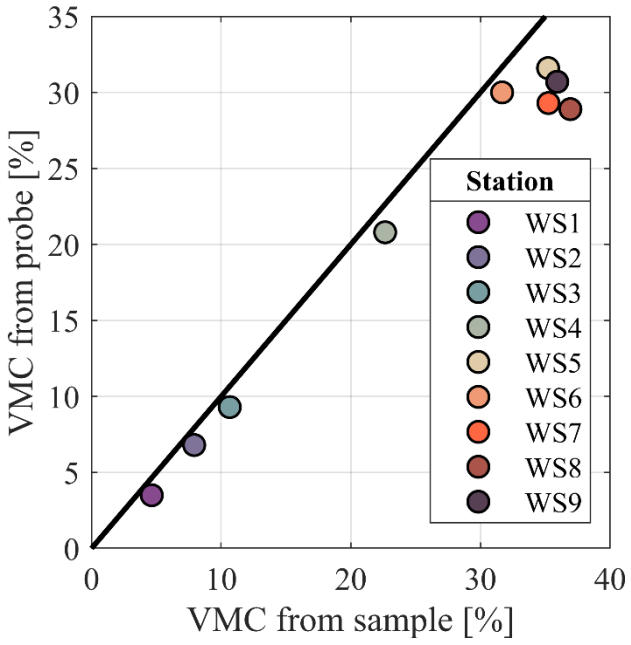


Figure 7. Relationship between the volumetric moisture content (VMC) from the soil samples and the moisture probe.

© ASCE

Beyond differences in the dry unit weights and variations in grain size, the salinity and composition of the water also causes discrepancies between the volumetric moisture content measured from the soil samples and the moisture probe. At most beaches, there are likely differences in the salinity between the backshore and the foreshore. This difference is further exacerbated by rainfall, where a greater volume of low-saline water is input into the sand. During measurements, a small amount of rainfall was observed, which may have impacted the measurements recorded by the probe. Future work will focus on co-located measurements of the moisture probe and porewater salinity to understand the impact on the measured moisture content/

CONCLUSION

This study investigated if a single set of calibration constants can be used to estimate the moisture content across different beach zones with different densities. Conductivity moisture probe measurements were paired with carefully collected sediment samples. The dry unit weight, grain sizes, and volumetric moisture contents were measured for each soil sample. Dry unit weights (ranging from 14.5-16.9 kN/m^3, with lower values (14.5-15.0 kN/m^3) observed in the backshore and higher values (15.3-16.9 kN/m^3) within the foreshore and swash zone. All volumetric moisture contents from the probe were greater than those measured from physical sampling. Within the backshore, the moisture contents gradually increased, with the volumetric moisture contents from the probe and sample exhibiting similar values (differences of 1.0-1.3%). Samples from the foreshore, however, had overestimates ranging from 0.9-7.1% and higher dry unit weights than the backshore, highlighting the role of dry unit weight on moisture probe calibration. The only station from the foreshore where a reasonable match was observed was WS6, where the dry unit weight was 15.6 kN/m3. However, this station exhibited a notable coarsening with depth (Figure 5), suggesting that sediment layering and variation in grain size may impact moisture contents recorded using moisture probes. Future work will focus on evaluating the role of sediment density, grain size, and sediment layering on the volumetric moisture contents recorded using moisture probes.

ACKNOWLEDGEMENTS

The authors would like to acknowledge the Office of Naval Research (ONR) for supporting this work though grant N00014-23-1-2414. They would also like to acknowledge Melissa Marry (UNH) for assisting with field measurements.

REFERENCES

ASTM. 2017a. *Standard Test Methods for Particle-Size Distribution (Gradation) of Soils Using Sieve Analysis*. ASTM D6913. ASTM International, West Conshohocken, PA, 04 (Reapproved 2009): 1–35.

ASTM. 2017b. *Standard Practice for Classification of Soils for Engineering Purposes (Unified Soil Classification System),* ASTM D2487-17. ASTM International, West Conshohocken, PA, USA, D2487-17: 1–10.

© ASCE

Atherton, R. J., A. J. Baird, and G. F. S. Wiggs. 2001. “Inter-Tidal Dynamics of Surface Moisture Content on a Meso-Tidal Beach.” *Journal of Coastal Research*, 17 (2): 482–489. Coastal Education & Research Foundation, Inc.

Brilli, N. C., N. Stark, B. Raubenheimer, S. Elgar, and B. Korka. 2022. “A simple laboratory calibration method for mitigating seawater effects on soil moisture sensors.” *Proceedings of the Coastal Engineering Conference*.

Davidson-Arnott, R. G. D., Y. Yang, J. Ollerhead, P. A. Hesp, and I. J. Walker. 2008. “The effects of surface moisture on aeolian sediment transport threshold and mass flux on a beach.” *Earth Surface Processes and Landforms*, 33 (1): 55–74.

Delta-T Devices Ltd. 2016. *User Manual for the SM150T*.

Heathershaw, A. D., A. P. Carr, M. W. L. Blackley, and C. F. Wooldridge. 1981. “Tidal variations in the compaction of beach sediments.” *Marine Geology*, 41 (3–4): 223–238.

Hillel, D. 1998. *Environmental Soil Physics*. Cambridge, M.A: Academic Press.

Lambe, T. W., and R. V. Whitman. 1969. *Soil Mechanics*. Hoboken, N.J.: John Wiley and Sons.

Namikas, S. L., B. L. Edwards, M. C. A. Bitton, J. L. Booth, and Y. Zhu. 2010. “Temporal and spatial variabilities in the surface moisture content of a fine-grained beach.” *Geomorphology*, 114 (3): 303–310. Elsevier B.V.

Paprocki, J., N. Stark, H. C. Graber, H. Wadman, and J. E. McNinch. 2022. “Assessment of moisture content in sandy beach environments from multispectral satellite imagery.” *Canadian Geotechnical Journal*, 59 (2): 225–238.

Paprocki, J., N. Stark, and H. Wadman. 2023. “A Framework for Assessing the Bearing Capacity of Sandy Coastal Soils from Remotely Sensed Moisture Contents.” *J. Geotech. Geoenviron. Eng.*, 149 (10): 04023083.

Schmutz, P. P., and S. L. Namikas. 2011. “Utility of the Delta-T Theta Probe for Obtaining Surface Moisture Measurements from Beaches.” *Journal of Coastal Research*, 27 (3): 478.

Tuttle, S. D. 1960. “Evolution of the New Hampshire shore line.” *Geological Society of America Bulletin*, 71 (8): 1211–1222. Geological Society of America.

Ward, L., N. Corcoran, Z. McAvoy, and R. Morrison. 2021a. *Seasonal Changes in Sediment Grain Size of New Hampshire Atlantic Beaches*.

Ward, L., K. McPherran, Z. McAvoy, and M. Vallee-Anziani. 2016. *New Hampshire Beaches: Sediment Characterization*.

Ward, L., R. Morrison, A. Eberhardt, W. Costello, Z. McAvoy, and C. Mandeville. 2021b. *Erosion and Accretion Trends of New Hampshire Beaches from December 2016 to March 2020: Results of the Volunteer Beach Profile Monitoring Program*.

Wiggs, G. F. S., A. J. Baird, and R. J. Atherton. 2004. “The dynamic effects of moisture on the entrainment and transport of sand by wind.” *Geomorphology*, 59 (1–4): 13–30.

Yang, Y., and R. G. D. Davidson-Arnott. 2005. “Rapid Measurement of Surface Moisture Content on a Beach.” *Journal of Coastal Research*, 213 (213): 447–452.

Zhu, Y. 2007. *Modeling Spatial and Temporal Variations of Surface Moisture Content and Groundwater Table Fluctuations on a Fine-Grained Beach, Padre Island, Texas*. Louisiana State University.

© ASCE

Evaluating the Efficacy of Instrumented Settlement Plates (ISP) in Monitoring Geotechnical Properties of Dredged Sediments in Marsh Creation Projects

Omar Snosi, S.M.ASCE[1]; and Navid Jafari, Ph.D., F.ASCE[2]

[1]Dept. of Civil and Environmental Engineering, Texas A&M Univ. (corresponding author).
ORCID: https://orcid.org/0009-0007-8933-7855. Email: omar.snosi@tamu.edu
[2]Dept. of Civil and Environmental Engineering, Texas A&M Univ.

ABSTRACT

Rapid wetland loss in coastal Louisiana necessitates effective marsh restoration through dredged sediment placement. However, current sediment management practices depend largely on laboratory-based predictions, which often lack field validation, resulting in uncertainties and conservative designs. This study evaluates in situ sediment behavior using Instrumented Settlement Plates (ISPs) deployed in two marsh creation projects (Bayou Bonfouca and Lost Lake), which provided continuous measurements of settlement and pore-water response. Results show that consolidation and zone settling behavior are strongly linked to sediment plasticity, with highly plastic, organic-rich clays consolidating more slowly than sandy, low-plasticity sediments. In addition, dredging and dewatering rates influenced settlement progression and dredge volume management. While ISPs proved valuable for tracking consolidation trends, they were not sufficient alone to fully characterize sediment behavior, underscoring the need to integrate complementary monitoring tools.

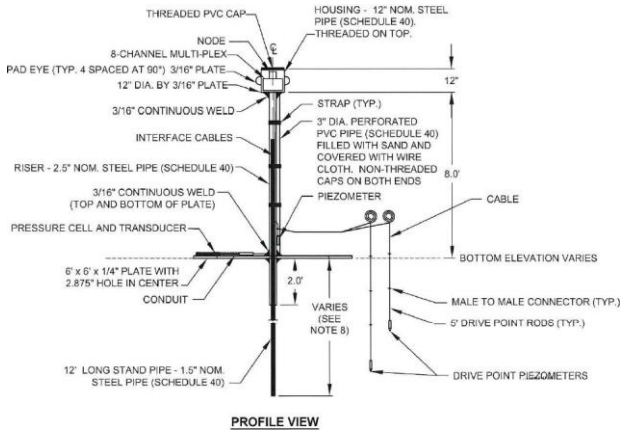
INTRODUCTION

Coastal Louisiana faces critical challenges due to rapid wetland loss, which threatens essential ecological functions and natural storm protection (Day et al., 2020). In response, Louisiana's Coastal Master Plan emphasizes marsh creation projects that utilize dredged sediment to restore degraded marshlands (CPRA, 2017). These restoration projects rely heavily on large-scale hydraulic dredging, where substantial sediment volumes are transported from borrow areas and hydraulically placed within targeted marsh creation sites.

Currently, dredging projects typically involve significant volumes of fill soil sourced from borrow areas. For instance, marsh creation projects like Bayou Bonfouca and Lost Lake required borrow volumes of approximately 3.6 million cubic yards and 5.4 million cubic yards, respectively (CPRA, 2021). Such extensive volumes underscore the necessity for efficient management of sediment placement operations to optimize dredging efficiency, manage fill volumes, and ensure long-term stability of created marshlands.

ISPs, illustrated in Figure 2 with (a) a schematic and (b) a field installation, provide continuous time series of base total stress and pore-water pressure within the sediment placed (CPRA, 2021). A crucial aspect of sediment management is accurately predicting post-placement behavior. Dredged sediment typically progresses through hindered settling, zone settling, and eventually self- weight consolidation as pore pressures dissipate and effective stresses develop (Sha et al., 2018; Stark et al., 2005). Current design practice, such as the U.S. Army Corps of Engineers' guidance (EM 1110-2-5025), often assumes that soil formation occurs at approximately half of the dredging duration (U.S. Army Corps of Engineers (USACE), 1987).

© ASCE

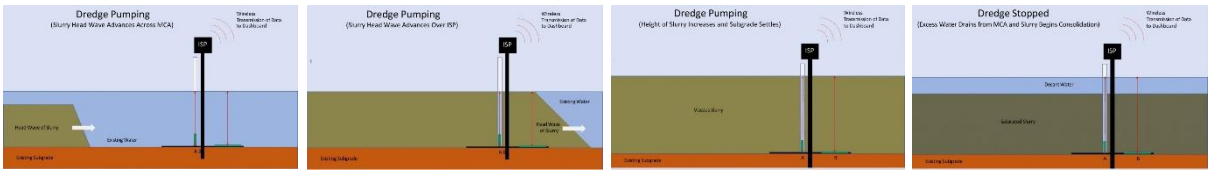




(a) ISP detailed section (schematic). **(b) Installed ISP in the field**

Figure 1. Instrumented settlement plate: (a) detailed section; (b) field photograph of an installed unit. (Source: CPRA, 2021)

However, such assumptions are derived primarily from laboratory column tests, which may not represent field-scale conditions and can result in conservative overbuilding (Morris et al., 2013). These processes control the dissipation of excess pore pressures, the development of effective stress, and ultimately the final marsh surface elevation and project performance (Harris et al., 2025).



(a) **(b)** **(c)** **(d)**

Figure 2. Stages of dredged sediment behavior observed using ISPs: (a) Decant and consolidation, (b) Slurry thickening and subgrade settlement, (c) Head wave passes ISP, and (d) Head wave advancing across the containment area. (Source: CPRA, 2021).

In this study, six ISP records were analyzed, three from the Lost Lake project (southwest of New Orleans) and three from the Bayou Bonfouca project (northeast of New Orleans). These instruments were used to reconstruct the applied loading during construction, including the timing and duration of lifts and pauses, and to evaluate how load rate and soil type influenced settlement of the marsh foundation. The loading signatures identified in the ISP data were validated against more than five hundred daily dredging production reports documenting placed quantities at the two sites, ensuring that stress changes captured by the ISPs aligned with actual construction operations.

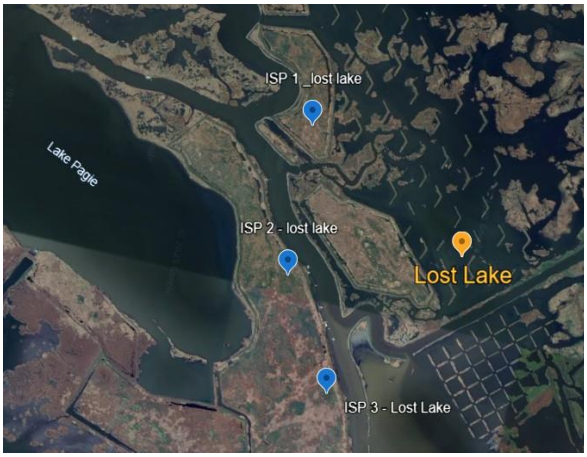
OBJECTIVES

The objective of this study is to clarify the role of ISPs in monitoring and managing dredged sediment behavior during marsh creation. The work is centered on two main goals:

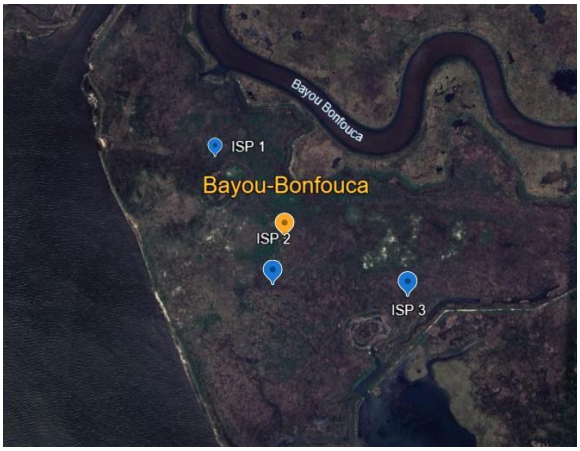
© ASCE

1. **Analyze ISP loading trends.** Examine how ISP records capture the timing, duration, and magnitude of loads applied during dredging, and evaluate how these trends interact with the type of dredged material to influence consolidation and long-term foundation settlement.
2. **Assess ISP capability for management.** Evaluate whether ISP measurements alone provide sufficient information to guide dredging volume management and settlement prediction, or whether complementary data and methodological refinements are required for reliable field application.

By focusing on these objectives, the study seeks to establish ISPs not just as monitoring devices but as decision-support tools, directly linking dredging operations, soil behavior, and marsh foundation performance.



(a) ISP 1–3 at the Lost Lake marsh creation project.



(b) ISP 1–3 at the Bayou Bonfouca marsh creation project.

Figure 3. (ISP installations locations).

METHODOLOGY

The 6 ISPs records were time-synchronized to construction logs and assembled into a unified database for analysis of loading history, pore-pressure response, and settlement implications.

ISP time series were pre-processed to remove offsets and establish consistent baselines prior to dredging. To account for background hydrologic variability, each record was integrated with water-level data from the nearest Coastwide Reference Monitoring System (CRMS) stations. This step ensured that observed pore-pressure fluctuations could be distinguished between natural water-level changes and loading effects from dredging.

Daily construction reports were then compiled and matched to the ISP timelines to identify the onset, duration, and pauses of loading. In total, 231 daily reports at Lost Lake and 214 at Bayou Bonfouca were used to confirm stress increases at the plates, refine the timing of individual lifts, and quantify rest intervals.

Borrow material data from project geotechnical reports, including gradation, Atterberg limits, and organic content, were used to classify dredged sediments and assign material parameters. Where spatial variability within a site was documented, descriptors were associated with the nearest ISP to preserve local context and enable comparison of soil-type effects on consolidation.

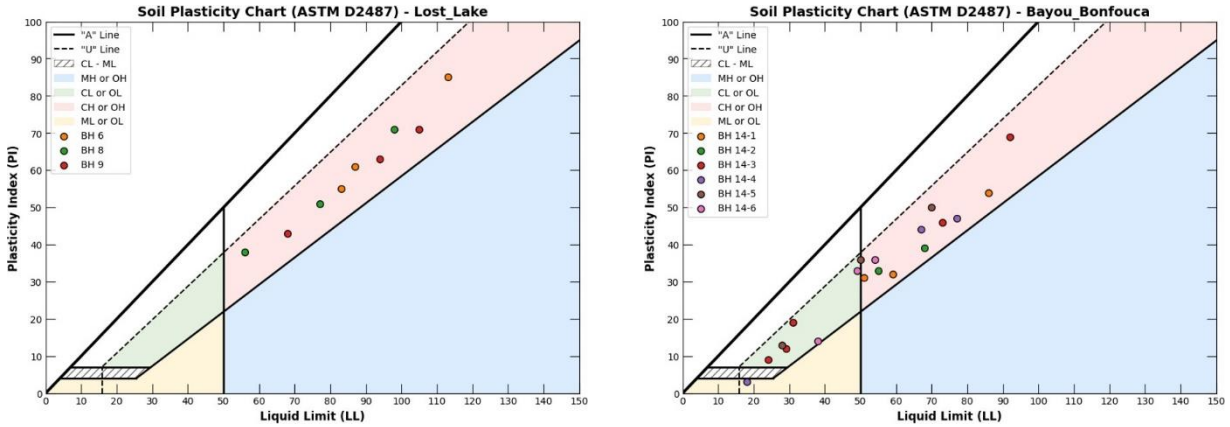
© ASCE

Finally, ISP-derived loading histories, and dredging soil properties were used as inputs to PSDDF (Primary, Secondary, and Desiccation Deformation of fine-grained soils) Stark et al. (2005). PSDDF provides a one-dimensional, finite-strain consolidation framework that accommodates staged loading, time-dependent compressibility–permeability behavior, secondary compression, and the evolution of the placed fill. For cross-project comparison, the foundation profile was generalized to a representative stratigraphy, while each site retained its measured loading durations, lift pacing, and dredged-material properties. Model outputs included settlement versus time for the foundation and the placed fill, early-time settlement rates, and times to reach selected fractions of final settlement. These results were used to evaluate how loading duration and material type influence settlement and to assess whether ISP records alone provide sufficient information for dredge volume management or if complementary measurements are required for reliable decision- making.

RESULTS

Dredged-Material Plasticity

Figure 4 compares the Atterberg-based plasticity of the placed materials at the two projects. Spec- imens from **Bayou Bonfouca** cluster at lower plasticity index (PI) and include a noticeable sand fraction; in contrast, **Lost Lake** specimens are markedly more plastic and organic. Practically, Bayou Bonfouca's lower PI implies higher hydraulic conductivity and faster pore-pressure dissi- pation; Lost Lake's higher PI indicates slower dissipation and larger long-term volumetric strains under similar loads. These material contrasts set the stage for site-specific consolidation behavior observed in the ISP and PSDDF results.



(a) Lost Lake **(b) Bayou Bonfouca**

Figure 4. Plasticity index (PI) charts for (a) Lost Lake and (b) Bayou Bonfouca.

ISP Time-Series: Placement, Pauses, and Dewatering

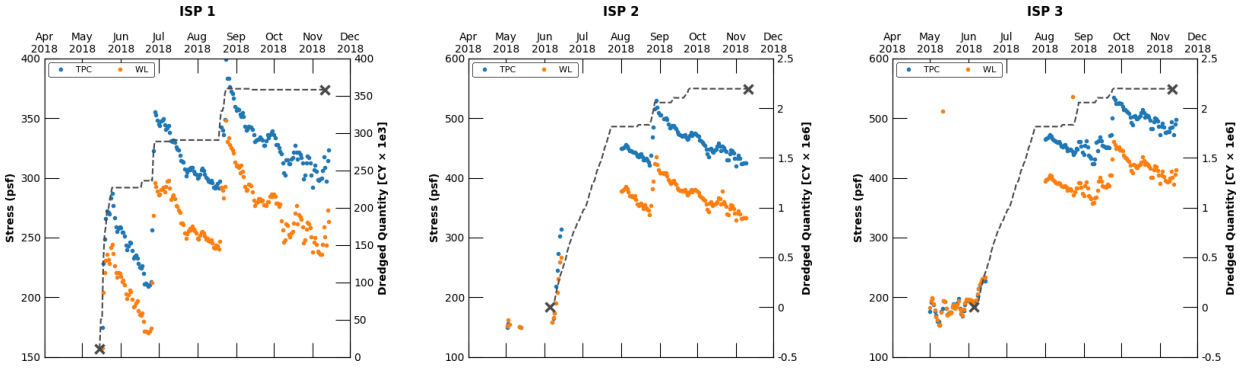
Figures 5 and 6 present the six ISP time-series grouped by project. Each panel overlays the Total Pressure Cell (TPC) and piezometer (WC) responses (CRM-calibrated prior to dredging) with daily production on a secondary axis. Across all instruments, step-wise increases in TPC align with lift placement; plateaus correspond to pauses; and WC rises during active placement then dissipates during pauses and dewatering episodes.

© ASCE

Lost Lake (Fig. 5): (a) TPC records distinct lift-related step-ups followed by gentle post-lift creep, reflecting gradual stress transfer as excess pore water pressures bleed; (b) WC exhibits pro- longed dissipation tails between lifts and after dewatering, consistent with the higher-PI material and lower hydraulic conductivity; (c) dewatering generates sharp WC drawdowns with contempo- raneous inflections in TPC. Overall, characteristic times between lift application and pore-pressure equalization are longer.

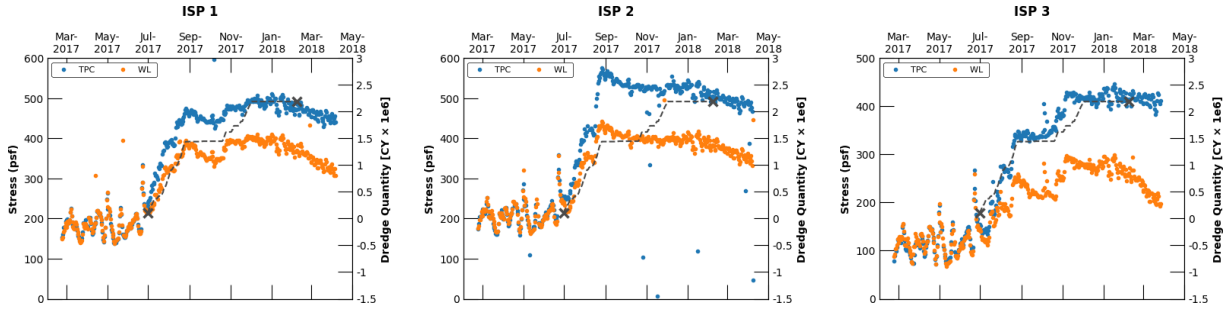
Bayou Bonfouca (Fig. 6): (a) TPC transitions are quicker with shorter inter-lift plateaus;

(b) WC decays more rapidly following each lift and during dewatering, indicating faster drainage pathways through the sandier matrix; (c) the system reaches quasi-steady response sooner between lifts, with smaller post-lift creep in TPC. In sum, effective stress builds faster at Bayou Bonfouca for comparable placed volumes.



(a) Lost Lake — ISP1 **(b) Lost Lake — ISP2** **(c) Lost Lake — ISP3**

Figure 5. Lost Lake ISP time-series (TPC, WC, and daily production).



(a) Bayou Bonfouca — ISP1 **(b) Bayou Bonfouca — ISP2** **(c) Bayou Bonfouca — ISP3**

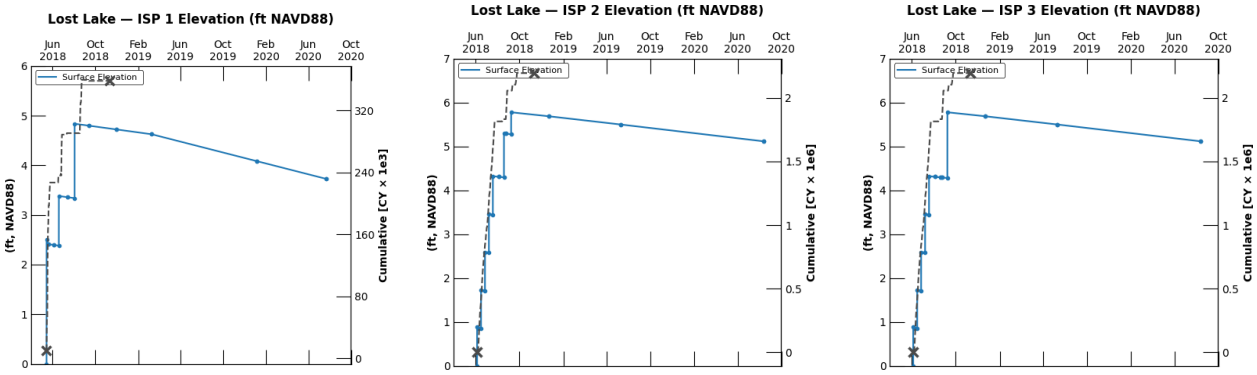
Figure 6. Bayou Bonfouca ISP time-series (TPC, WC, and daily production).

Settlement Magnitudes and Durations from PSDDF

Figures 7 and 8 show settlement histories reconstructed via PSDDF for the same instruments. Two features are consistent across records: (1) settlement increases in discrete increments synchronous with lifts and continues at diminishing rates during pauses (primary consolidation followed by secondary creep); (2) material control is evident—Lost Lake develops larger total settlement and requires longer durations to approach stabilization, whereas Bayou Bonfouca stabilizes sooner at smaller magnitudes for comparable placed volumes.

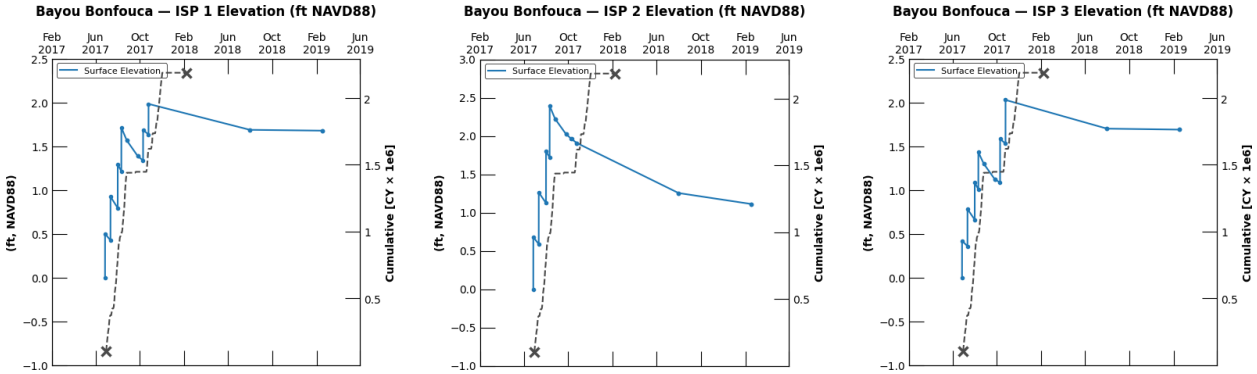
© ASCE

Within Lost Lake, successive lifts superimpose new primary consolidation on still-active dissipation from prior lifts, producing extended shoulders in the PSDDF curves. Within Bayou Bonfouca, later lifts add measurable settlement but with shorter tails; the higher-permeability fabric reduces inter-lift interaction among excess pore pressures.



(a) Lost Lake — ISP1 **(b) Lost Lake — ISP2** **(c) Lost Lake — ISP3**

Figure 7. Lost Lake PSDDF-derived settlement histories.



(a) Bayou Bonfouca — ISP1 **(b) Bayou Bonfouca — ISP2** **(c) Bayou Bonfouca — ISP3**

Figure 8. Bayou Bonfouca PSDDF-derived settlement histories.

CONCLUSION

The results highlight the joint influence of dredge material properties and placement history on consolidation response in marsh creation projects. At Lost Lake, the three ISPs recorded two distinct placement styles. ISP1, located in MCA 1A, was loaded in three rapid lifts within only a few days. ISP2 and ISP3, located in MCA B, each received two lifts: the first applied gradually over nearly a month, the second placed rapidly within days. Despite these operational differences, all Lost Lake sites were characterized by high-plasticity, organic dredge that produced long dissipation times and extended consolidation tails. Stabilization was therefore slow and settlement magnitudes were moderate.

At Bayou Bonfouca, placement was slower overall but more spatially variable. ISP1 received its first lift over 43 days and a smaller second lift three weeks later. ISP2 experienced essentially one major lift over a month at a higher applied stress. ISP3 recorded two lifts, the first over 44

© ASCE

days and the second about four weeks later, both producing relatively large magnitudes. This spatial variability in placement sequencing is consistent with project reports of clay ball formation, which created irregular dredge delivery across the site. The ISP records capture these differences as variations in the number, magnitude, and timing of TPC step-ups.

The settlement implications are clear. Lost Lake, with its more plastic, organic dredge, dissipated pore pressures slowly and required longer durations to stabilize, but exhibited smaller overall settlements. Bayou Bonfouca, with a sandier, lower-PI dredge, consolidated more quickly. However, the largest settlement occurred at Bayou Bonfouca ISP2, where nearly the full load was applied in a single lift. This outcome underscores the importance of placement sequencing: loading soils in multiple smaller lifts can reduce ultimate strain compared to one large lift, even in faster-draining materials.

In practice, these findings emphasize that both *soil plasticity* and *lift sequencing* govern consolidation trajectories. High-PI dredge, such as at Lost Lake, will prolong stabilization regard- less of placement style, while lower-PI, sandier dredge, such as at Bayou Bonfouca, will dissipate rapidly but may settle substantially if loading is concentrated in a single event. Recognizing these interactions can inform operational strategies for marsh creation, including the timing and size of lifts, to better control settlement magnitude and duration.

LIMITATIONS AND FUTURE WORK

While the ISP records provided valuable insights into dredge placement, pore-pressure dissipation, and settlement progression, several limitations remain. First, piezometer readings are highly sensitive to the surrounding medium. During slurry placement, the instrument tip is immersed in a fluid denser than water, leading to apparent water levels that overestimate the true phreatic surface. As deposition proceeds, the tip transitions into a soft, saturated mud layer where excess pore pressures dominate the signal. Only after full consolidation do the readings correspond directly to pore water pressure. Consequently, interpreting piezometer data as a continuous indicator of water level or zone-settling behavior can be misleading.

Second, the ISP framework alone cannot unambiguously identify the transition from ac- tive slurry to the onset of self-weight consolidation. This transition—the “zone-settling” pe- riod—controls both the efficiency of dredging operations and the volume ultimately required to achieve design grade. The Lost Lake project illustrates this challenge: premature dewatering likely commenced while excess pore pressures were still elevated, prolonging dissipation and increasing the total fill volume needed.

Future work should therefore focus on integrating ISPs with a complementary monitoring device capable of directly tracking the elevation and thickness of newly settled sediment layers. In real time. Such a tool would allow operators to initiate dewatering only after the true settling zone has been established, avoiding premature drainage in high-plasticity deposits. From a re- search standpoint, combined measurements of pore pressure, effective stress, and evolving deposit geometry would enable more accurate evaluation of consolidation models and improve predictive frameworks for zone-settling duration beyond current empirical assumptions.

REFERENCES

CPRA. (2017). “Louisiana’s comprehensive master plan for a sustainable coast.” Report no., CPRA, Baton Rouge, LA.

© ASCE

CPRA. (2021). “Bayou bonfouca marsh creation project completion report.” Report no., Coastal Protection and Restoration Authority, Baton Rouge, LA.

Day, J. W., Shaffer, G. P., Britsch, L. D., Reed, D. J., Hawes, S. R., and Cahoon, D. (2020). “Patterns and processes of wetland loss in coastal louisiana.” *Estuaries and Coasts*, 43(7), 1723–1745.

Harris, B. D., Shawler, J. L., and Turner, R. E. (2025). “Predicting elevation change in marsh creation projects: a comparison of laboratory and field data.” *Journal of Coastal Research*, 41(3), 289–301.

Morris, J. T., Sundareshwar, P. V., Nietch, C. T., Kjerfve, B., and Cahoon, D. R. (2013). “Responses of coastal wetlands to rising sea level.” *Ecology*, 83(10), 2869–2877.

Sha, X., Jafari, N. H., Stark, T. D., and Harris, B. D. (2018). “Sedimentation and consolidation behavior of fine-grained dredged material in column tests.” *Journal of Geotechnical and Geoenvironmental Engineering*, 144(12), 04018102.

Stark, T. D., Choi, H., and Schroeder, P. R. (2005). “Settlement prediction for dredged material placement areas.” *Journal of Geotechnical and Geoenvironmental Engineering*, 131(1), 78–88.

USACE. (1987). “Engineering and design – confined disposal of dredged material.” Report No. EM 1110-2-5025, US Army Corps of Engineers, Washington, D.C.

© ASCE